



The multi scenarios applicability of GNSS differential positioning technology in the remeasurement of observatory azimuth angles

Yufei He¹, Xudong Zhao¹, Suqin Zhang¹, Qi Li¹, Fuxi Yang², Shaopeng He³ and Pengkun Guo³

¹Institute of Geophysics, China Earthquake Administration, Beijing, 100081, China

²Xinjiang Earthquake Administration, Urumqi, 830011, China

³Hebei Earthquake Administration, Shijiazhuang, 230071, China

Correspondence to: Xudong Zhao (zxd9801@163.com)

Abstract. The azimuth angle of geomagnetic observatory markers is crucial for ensuring the reliability of geomagnetic observation data, and its remeasurement constitutes a core task in observatory operations. By comparing the precision, efficiency, and environmental adaptability of astronomical observation methods and GNSS differential positioning techniques for azimuth measurement, this study reveals that traditional astronomical methods suffer from significant environmental constraints and low efficiency compared to GNSS differential positioning technology. After systematically investigating the multi scenarios in azimuth remeasurement at geomagnetic observatories, five remeasurement scenarios based on GNSS differential positioning technology are proposed, addressing practical conditions such as unobstructed paths, restricted pathways, and single point deployments. Through field validations at the Hongshan, Quanzhou, and Yulin observatories, the feasibility of Scenario I (dual GNSS deployment on unobstructed paths) and Scenario II (multi path angles conversion) is confirmed. Field validations at Hongshan, Quanzhou, and Yulin observatories confirmed the feasibility of Scenario I (dual-GNSS deployment on unobstructed paths) and Scenario II (angular conversion across paths). Furthermore, a preliminary analysis was conducted on potential error sources in different scenarios, and a prioritized implementation sequence was established for stations that simultaneously meet the conditions of each retest scenario. This work provides a scalable technical solution for azimuth measurement in complex geomagnetic observatories environments.

1 Introduction

The geomagnetic field, as a fundamental physical field of Earth, not only protects biological evolution but also serves as a key parameter in geoscientific exploration. Geomagnetic observatories, designed for long term continuous monitoring of geomagnetic variations (Jankowski and Sucksdorff, 1996), acquire seven components vector data—total intensity (F), horizontal component (H), declination (D), inclination (I), and Cartesian coordinates (X/Y/Z). These data are extensively applied in deep resource exploration, high precision navigation, and space environment monitoring (Lu et al., 2022; Lin et al.,



2023; Zhang et al.,2024a). Ensuring the precision and accuracy of absolute geomagnetic observations is of paramount importance (Zhang et al.,2024b).

It is essential to emphasize that the absolute measurement of the seven geomagnetic components at observatories is achieved through a collaborative system comprising relative recorders and absolute observation devices (St-Louis et al.,2024; Bracke et al., 2025). The relative recorders enable continuous monitoring with a sub second sampling rate, while the absolute observations calibrate baseline values periodically via manual or automated methods (currently focusing on D/I/F components twice weekly). The integration of both systems produces continuous absolute observation data with minute level temporal resolution and accuracy better than 1 nT (Zhang et al., 2016). Consequently, the frequency and precision of absolute observations directly determine baseline reliability, which in turn impacts the quality of final data—this represents the key technical bottleneck in enhancing the accuracy of absolute geomagnetic observations within the current monitoring framework.

The magnetic declination (D), defined as the angle between the geomagnetic field direction and true north, is particularly critical for practical applications such as oil drilling and navigation (Shi et al., 2008; Li et al., 2023). Currently, the measurement of magnetic declination (D) at geomagnetic observatories is primarily conducted using fluxgate theodolites instruments (abbreviated as DI instruments), in conjunction with the azimuth angle of the observatory's reference markers. Consequently, the accuracy of the azimuth angle is fundamentally vital to the reliability of these measurements.

The azimuth marker is one of the critical core facilities at geomagnetic observatories, and the azimuth angle (i.e., the angle between the line connecting the center of the observation pillar to the center of the marker and the true north direction) is also a vital parameter. Typically, the construction of azimuth markers requires long term stability and robustness (CEA, 2004). When feasible, the markers should ideally be engraved or built directly onto bedrock. The measurement of the azimuth angle is generally completed during the observatory's construction phase (Zhou et al.,1997; Xu et al., 2003; Yang et al., 2008; Wang et al., 2014;). If the absolute observation chamber of the observatory has not yet been roofed, the azimuth angle can be directly measured at the center of the observation pillar using either astronomical observation methods (Ma, 1995; Cheng et al., 1996; Liu et al., 2020; Khanzadyan and Mazurkevich, 2021) or GNSS differential positioning technology (Yin et al., 2008; Zhou et al., 2009; Li et al., 2015; Yu et al., 2018). The azimuth marker and angle are put into service simultaneously with the commencement of the observatory's operations.

The construction of azimuth markers requires long term stability. However, over extended periods of operation at geomagnetic observatories, these markers may undergo displacement due to natural environmental changes or human induced disturbances. For instance, geological tectonic activities (e.g., earthquakes), crustal deformation, or subsurface fluid movements could shift observation pillars. Similarly, urban expansion—such as the construction of large scale facilities nearby, urban loading, or groundwater extraction—may lead to tectonic deformation, causing positional changes in the azimuth markers. Therefore, periodic remeasurements of the marker azimuth angles are essential in geomagnetic observatory operations to verify accuracy and promptly correct errors, thereby ensuring the reliability and precision of geomagnetic data. Azimuth angle remeasurement is a core procedure for maintaining data quality. Consequently, China's geomagnetic observatory operational guidelines



explicitly mandate azimuth angle remeasurements every 10 years, with additional assessments required immediately if significant changes in the markers are detected (CEA, 2001).

65 The study first provides a concise introduction to two methods for measuring marker azimuth angles, followed by a comparative analysis. It further examines multi scenarios applicability across diverse geomagnetic observatory environments and proposes five remeasurement schemes based on GNSS differential positioning technology. Field validations at multiple observatories demonstrate the frameworks' effectiveness, offering methodological references for azimuth remeasurement protocols

70 2 Azimuth measurement methods

Currently, geomagnetic observatories primarily use two methods for azimuth measurement: Astronomical Observation and GNSS Differential Positioning. Early observatories predominantly adopted astronomical observation, while newer ones widely employ GNSS differential positioning.

2.1 Astronomical observation method

75 This method relies on the relationship between celestial bodies (e.g., the Sun, Polaris, stars) and Earth's rotation. By calculating the true north direction of a celestial body and measuring its horizontal angle with a ground target, the azimuth angle is determined (SBQTS, 2000). As shown in Fig. 1, the spherical relationship involves the observation point O, ground marker M, projection S' of celestial body S, and the North Celestial Pole P. To calculate the azimuth angle a_{NM} , the horizontal angle θ between the celestial body and the marker is measured, and the celestial azimuth A is derived from the observation time:

$$a_{NM} = A + \theta \quad (1)$$

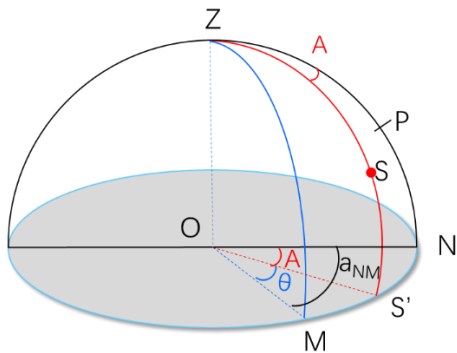


Figure 1: Spherical Diagram of Astronomical Azimuth



Equation (1) indicates that the azimuth angle of the ground marker equals the sum of the celestial azimuth and the horizontal angle. For Polaris measurement, the formula for A (measured eastward from true north) is derived from the spherical triangle (Fig. 2):

$$A = \tan^{-1} \left(\frac{\sin t}{\cos \varphi \tan \delta - \sin \varphi \cos t} \right) \quad (2)$$

Here, φ is the observer's latitude, δ is Polaris' declination, and t is the hour angle. The determination of azimuth angles using Polaris constitutes the most widely adopted method in astronomical azimuth measurement, capable of fulfilling diverse precision requirements. While this celestial observation technique eliminates reliance on electronic equipment, making it suitable for remote areas or GNSS denied environments, the measurement process exhibits significant dependencies on weather conditions and visibility. However, its operational efficiency is constrained by significant dependencies on favorable meteorological conditions, coupled with requirements for specialized expertise, computationally intensive procedures, and prolonged observation durations.

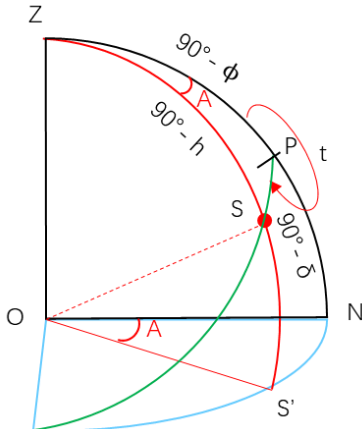


Figure 2: Spherical position triangle

2.2 GNSS differential positioning method

The GNSS differential positioning method employs two stationary receivers (one serving as a base station and the other as a rover) to conduct synchronized prolonged continuous observations. Through post processing error elimination and baseline resolution, this technique acquires high precision three dimensional coordinates for both measurement points (A and B). Then transforming coordinates of A and B into a common planar coordinate system (e.g., UTM or local independent coordinate system) following IGS standards. Finally, the azimuth angle is derived from the planar coordinates of reference point (A) and target point (B), using the arctangent function:

$$A = \tan^{-1} \left(\frac{E_B - E_A}{N_B - N_A} \right) \quad (3)$$



105 where E and N represent easting and northing coordinate differences respectively. This method provides near real time results and is weather independent, but signal obstructions or multipath effects (e.g., near water or reflective surfaces) may degrade accuracy.

This method demonstrates rapid implementation and near real time result acquisition, achieving weather independent operation with all weathers capability, thus exhibiting enhanced operational efficiency. While extending observation duration improves
110 single point positioning accuracy, its performance degrades significantly in signal deprived or obstructed environments, with positioning errors exacerbated by multipath effects (notably near water surfaces, glass curtain walls, and metallic reflective surfaces).

Table 1 summarizes the key characteristics of both methods. Their complementary advantages in precision, environmental adaptability, and application scenarios allow combined use for enhanced reliability.

115

Table 1: Comparison of Azimuth Measurement Methods

Method	Astronomical Observation	GNSS Differential Positioning
Equipment	Theodolite, ephemeris, timer	Dual GNSS receivers, data processing software
Limitations	Requires clear skies or visible celestial body	Requires open sky, susceptible to obstructions
Complexity	High (astronomy expertise needed)	Low (automated)
Precision	0.5" (Polaris based first class measurement)	1"~2" (ideal conditions)
Applications	Remote areas, military operations, heritage restoration	Engineering survey, UAV navigation, traffic planning
Error Sources	Atmospheric refraction, timing errors, instrument alignment	Multipath effects, ionospheric delay, satellite geometry
Timeliness	Delayed (post processing)	Real time/near real time

3 Multi scenarios analysis for azimuth remeasurement

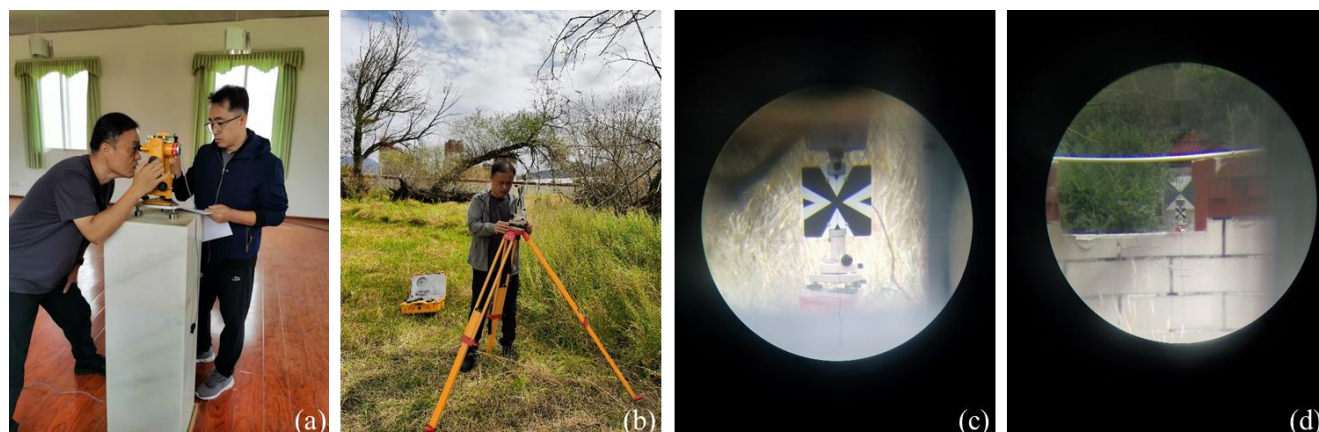
The original marker azimuths of geomagnetic observatories are typically measured during or immediately after construction
120 (before the completion of observatory walls and roofs) to ensure accuracy. Most stations continue to use the initial values, while some require remeasurements due to marker relocations or environmental changes. Given that many stations have operated for over a decade, and that early azimuth markers were constructed under non uniform standards with diverse designs (as shown in Fig.3), remeasuring azimuths has become crucial. Both astronomical observations (based on Polaris) and GNSS differential positioning meet high precision requirements. However, GNSS is preferred for its efficiency, especially in China's
125 extensive observatory network. Current remeasurements face challenges such as signal obstruction by buildings or vegetation, necessitating adaptive solutions tailored to site specific conditions.



Figure 3: Different styles of azimuth markers

3.1 Scenario I: Flat and clear line of sight

- 130 If the path between the observation pillar in the geomagnetic absolute observation room and the azimuth marker is flat and unobstructed, and two GNSS receivers can be deployed along the line of sight (LOS), with no tall vegetation around them and sufficient separation (for GNSS receivers with a horizontal positioning error of 2 mm, a minimum distance of 200 m between them is required to achieve 2" level measurement accuracy), while ensuring that the targets of both GNSS receivers are visible from the observation pillar. When verifying this scenario, the GNSS devices should be installed along the unobstructed line of sight
- 135 sight path, ensuring sufficient distance between them. A high precision theodolite (1" level) must be used to align the azimuth marker and the two GNSS targets, guaranteeing that the center of the observation pillar, the azimuth marker, and both targets lie on a single straight line. As shown in Fig.4, images illustrate the alignment process from the observation pillar to the GNSS targets and the azimuth marker.



140 **Figure 4: Theodolite alignment to the GNSS targets and the azimuth marker.**



Figure 5 illustrates the schematic diagram for calculating the azimuth angle based on this method, where O represents the center of the observation pillar, A and B denote the two GNSS survey points, M is the azimuth marker, and a_{NM} and a_{GNSS} indicate the azimuth angles of the azimuth marker and the GNSS survey line, respectively (these symbols retain the same meaning in subsequent schematic diagrams and will not be reiterated in later sections). If the OM distance is sufficiently long to meet measurement requirements, points A and B can be installed between O and M, as shown in Fig. 5(a). However, if the distance between A and B is too short to satisfy measurement criteria, point B can be relocated beyond marker M to a farther position, as depicted in Fig. 5(b).

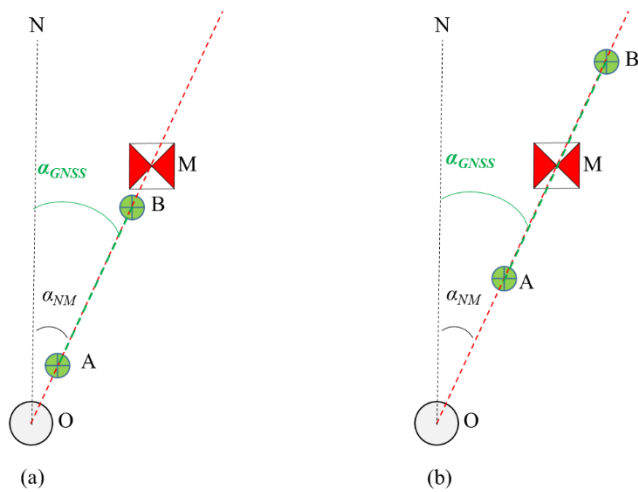


Figure 5: GNSS collinear deployment

As shown in Fig. 5, since points O, A, B, and M lie on the same straight line, the azimuth angle of the OM connection (a_{NM}) is identical to the azimuth angle of the line connecting the two GNSS survey points A and B (a_{GNSS}). In this scenario, the azimuth angle of the GNSS survey line is equivalent to that of the azimuth marker:

$$a_{NM} = a_{GNSS} \quad (4)$$

3.2 Scenario II: Alternative clear path available

When there is a clear line of sight between the observation pillar and the azimuth marker, but the path is obstructed by tall vegetation (which may interfere with GNSS satellite signal reception), or the terrain along the path is uneven (preventing visual alignment of targets from the pillar), or the path lacks sufficient distance to deploy two GNSS devices, an alternative survey line in another direction with clear visibility and sufficient length can be identified. In such scenarios, the GNSS devices can be deployed along this alternative survey line. By conducting GNSS measurements, the azimuth angle of this line can be determined. Subsequently, using a high precision theodolite (1" level) to measure the angle between this line and the azimuth marker's path, the azimuth angle of the marker can ultimately be derived. Figure 6 provides a schematic diagram of this measurement method.

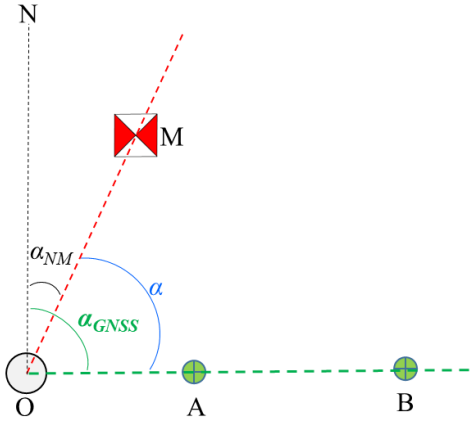


Figure 6: Alternative path GNSS deployment

165 As shown in Fig. 6, since points O, A, and B are collinear, the GNSS devices at A and B can measure the azimuth angle of this line (α_{GNSS}). The angle α between the OM line and the collinear line OAB can be determined through repeated measurements with a high precision theodolite (1" level). In this scenarios , the azimuth angle of the observation marker OM (α_{NM}) is derived via the following formula:

$$\alpha_{NM} = \alpha_{GNSS} - \alpha \quad (5)$$

170 3.3 Scenario III: Single GNSS receiver on LOS

When there is clear line of sight between the observation pillar and the azimuth marker, but insufficient distance or obstructions from tall vegetation prevents to deploy two GNSS devices along this direction, and only one GNSS setup is feasible. In such scenario, the following approach can be adopted. One GNSS device can be deployed along the path between the observation pillar and the azimuth marker. The second GNSS device can be placed on another path with clear mutual visibility to the first

175 GNSS unit, ensuring the distance meets measurement requirements. Then the azimuth angle of the GNSS baseline can be determined using GNSS differential methods. Subsequently, a high precision theodolite, mounted on the tripod at the first GNSS station, can be used to measure the angel between Point O (or Point M, depending on field setup constraints) and the GNSS target at Point B by conducting repeated measurements. The azimuth angle of the marker can be ultimately calculated using the two angels, as illustrated in Fig. 7.

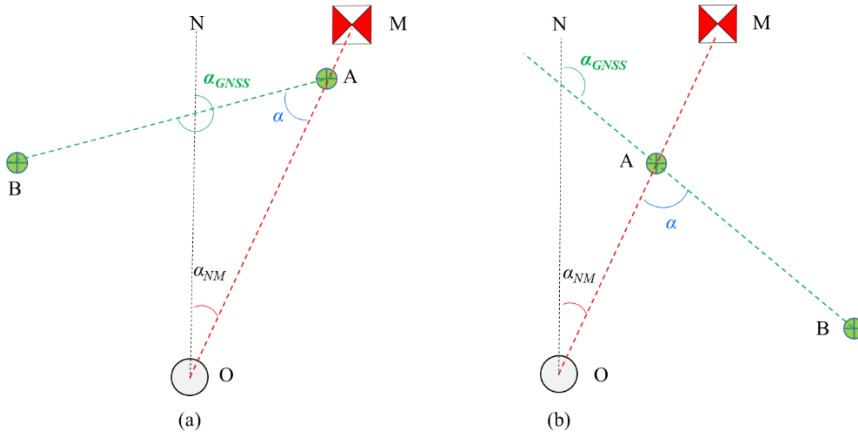


Figure 7: Single GNSS on main path (a) B is left of A (b) B is right of A

Figures 7(a) and (b) illustrate the two scenarios where Point B located to the left and right of Point A, respectively. Points O, A, and M are collinear. The azimuth angle of the baseline AB is denoted as α_{GNSS} . The angle between AB and AO is α . The azimuth angle of the marker (α_{NM}) can be calculated as follows:

$$a_{NM} = \begin{cases} a_{GNSS} - 180^\circ - \alpha, & (B \text{ is left of } A) \\ a_{GNSS} - (180^\circ - \alpha), & (B \text{ is right of } A) \end{cases} \quad (6)$$

3.4 Scenario IV: Single point visibility

If no suitable locations are available for deploying GNSS units along the direct path between the observation pillar and the azimuth marker, but an alternate point can be identified that maintains line of sight with both the observation pillar and another measurement point meeting distance requirements. The following workflow can be applied in this scenario. First, two GNSS units can be deployed at the two measurement points. The azimuth angle of the GNSS baseline connecting the two GNSS units can be measured using GNSS differential positioning. Subsequently, a high precision theodolite can be mounted at the GNSS station with visibility to the observation pillar. Through repeated measurements, the angular offset between the second measurement point and the center of the observation pillar is determined. The theodolite is then relocated to the observation pillar, where repeated measurements are conducted to obtain the angular offset between the azimuth marker and the visible measurement point. Finally, the azimuth angle of the azimuth marker is calculated based on the angular relationships derived from these measurements. A schematic diagram of the measurement process is illustrated in Fig. 8.

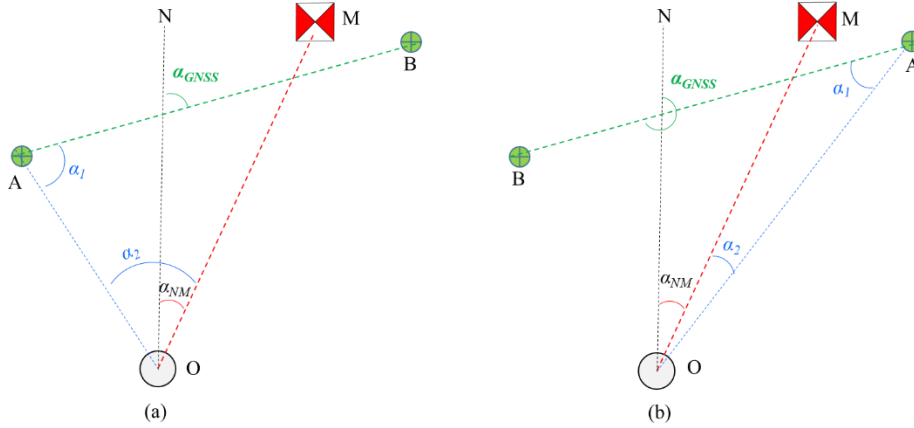


Figure 8. Single point visibility measurement (a) B is right of A (b) B is left of A

In Fig. 8, Point A is mutually visible to both the center of the observation pillar (O) and measurement point B. Figures 8(a) and (b) depict scenarios where Point B is positioned to the right and left of Point A, respectively. Here, a_{GNSS} denotes the azimuth angle measured by GNSS differential positioning, while α_1 and α_2 represent the angular offsets observed at Point A and the observation pillar. Based on the angular relationships illustrated in the figures, the azimuth angle of the azimuth marker is calculated as follows:

$$a_{NM} = \begin{cases} (a_{GNSS} - 180^\circ) - \alpha_1 - \alpha_2, & (B \text{ is left of } A) \\ a_{GNSS} - (180^\circ - \alpha_1 - \alpha_2), & (B \text{ is right of } A) \end{cases} \quad (7)$$

3.5 Scenario V: No GNSS deployment feasibility

If none of the preceding scenarios are applicable (i.e., no GNSS compatible locations exist within the line of sight range of the observation pillar in the observation room), but an auxiliary point can be identified that is both mutually visible to the observation pillar and aligned with a measurement line that meets GNSS deployment requirements. Then the remeasurements can be completed rely on the auxiliary mutually visible point.

Most historical geomagnetic observatories were equipped with calibration huts containing an observation pillar. This pillar was designed to maintain mutual visibility with the observation pillar in the main observation room and to offer clear sightlines to its surroundings (if Polaris could be observed from this pillar, astronomical azimuth methods could theoretically be applied, though this is not discussed here). If a specific direction near the pillar provides unobstructed visibility and meets the requirements for deploying two GNSS units, the pillar can serve as an auxiliary reference point. If such a pillar is not available at the station, a tripod can be set up at the location to act as a temporary auxiliary point.

In this scenario, a high precision theodolite is set up at the auxiliary point (either the observation pillar in the calibration hut or a tripod mounted location). The theodolite is aligned to ensure that the two GNSS measurement points lie on the same survey line. Through repeated measurements, the angular offset α_1 between the target marker of either GNSS station and the center O (marked by a fine needle secured with clay) of the observation pillar in the observation room is determined.



Subsequently, the high precision theodolite is relocated to the observation pillar inside the observation room, where repeated measurements yield the angular offset α_2 between the azimuth marker and the center P of the auxiliary point. Finally, by integrating the results from GNSS differential positioning, the azimuth angle of the azimuth marker can be calculated. Figure 9 illustrates a schematic diagram of this measurement method.

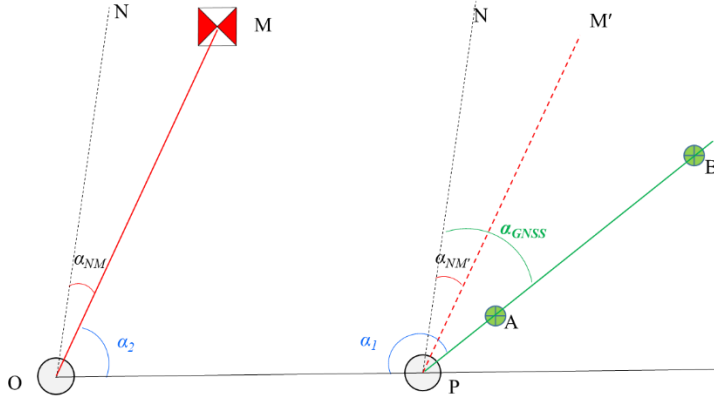


Figure 9. Indirect measurement via auxiliary point.

In Fig. 9, point P represents the center of the auxiliary measurement point (observation pillar or tripod setup), and PM' is the parallel line to OM . Thus, the azimuth angle α_{NM} equals $\alpha_{NM'}$. From the angular relationships shown in the figure, the azimuth angle of the marker can be derived as:

$$\alpha_{NM} = \alpha_{GNSS} - (\alpha_1 + \alpha_2 - 180^\circ) \quad (8)$$

4 Multi scenarios case studies in azimuth remeasurement

The previous text analyzed five potential scenarios for azimuth remeasurement and provided corresponding measurement solutions. Based on these scenarios, we have preliminarily initiated remeasurements at stations with long standing azimuth markers and obtained initial results. Currently, azimuth remeasurements have been completed at three stations: Hongshan Geomagnetic Observatory, Quanzhou Geomagnetic Observatory, and Yulin Geomagnetic Observatory.

Hongshan Geomagnetic Observatory, located in the North China Plain, started its previous azimuth marker in 2003 (22 years ago); the path between its observation pillar and azimuth marker features flat terrain with a completely unobstructed line of sight, satisfying Scenario I conditions, hence Scenario I methodology was adopted. Quanzhou Geomagnetic Observatory in southeastern China's hilly terrain has its azimuth marker engraved on bedrock, dating back to 2007 (18 years ago); although the path is complex, two measurement point meeting Scenario I requirements can be identified, so Scenario I was applied. Yulin Geomagnetic Observatory, located in the suburban area of Yulin, northwestern China, had its original primary azimuth marker destroyed. However, before its destruction, the azimuth angle was transferred to the rooftop of a distant building and has been in use since 2009 (16 years ago). Due to multiple buildings and tall trees obstructing the path, measurements using



245 Scenario I were unfeasible. Fortunately, an alternative survey line meeting Scenario II requirements was identified from the opposite side of the observation room, enabling azimuth remeasurement via Scenario II. Additionally, Scenario III methodology was also attempted, but measurement errors increased due to the short line of sight distance between compliant points. Detailed results for all three observatories are presented in Table 2.

Table 2. Comparison of remeasured and original azimuth angles

Observatory	Scenario	Pillar No.	Remeasured		Original		Deviation
			Azimuth	Method	Azimuth	Method	
Hongshan	I	1#	1° 31' 55.8"	GNSS	1° 31' 52.2"	Astronomy	3.6"
		2#	2° 22' 10.8"		2° 22' 9.6"		1.2"
Quanzhou	I	1#	179° 46' 37.9"	GNSS	179° 46' 28.6"	Astronomy	9.3"
		5#	178° 30' 34.4"		178° 30' 25.6"		8.8"
Yulin	II	1#	354° 49' 40.2"	GNSS	354° 49' 31.2"	Astronomy	9.0"
	III	1#	354° 48' 49.3"				41.9"

250 **5 Conclusions and discussion**

This paper briefly compares two current methods for measuring azimuth markers at geomagnetic observatories and proposes five applicable remeasurement scenarios based on GNSS differential positioning, comprehensively covering all remeasurement challenges. Comparative analysis reveals: Scenario I requires only device alignment (ensuring collinear points), simplifying operations without angular measurements or conversions, thus introducing no additional errors beyond four points alignment inaccuracies. Scenarios II and III necessitate measuring one angle (beyond alignment), introducing single error sources; however, Scenario II performs this measurement on more stable observation pillars, while Scenario III uses tripods, making Scenario II superior. Scenarios IV and V require measuring two angles (introducing dual errors), with one typically tripod based. If Scenario V employs a stable observation pillar as an auxiliary point, it outperforms Scenario IV. Consequently, remeasurement priority is ranked: Scenario I (optimal) > Scenario II > Scenario III > Scenario V (with fixed pier) > Scenario IV (unoptimized). Repeated measurements are advised for angle involving scenarios to minimize errors.

260 Field measurements at three observatories using Scenarios I–III confirm the feasibility of these remeasurement methods. While only three scenarios have been tested thus far, future work will expand measurements to quantify error magnitudes across all scenarios. Current tests of Scenario III yielded significant errors due to suboptimal conditions: insufficient distance between GNSS setup points and mandatory tripod based angle measurements outdoors. This underscores both the criticality of adequate baseline distances and the need for further error analysis of tripod based measurements. Nevertheless, we detected minor



azimuthal shifts—though numerically small, these findings enhance data accuracy assurance for observatory operations, validating the significance of this work.

270 Remeasurements show minimal azimuthal changes at all three stations: Quanzhou’s marker is engraved on bedrock; Hongshan’s marker is mounted on a pillar with a stable foundation on level ground; Yulin’s original mark was destroyed, and its marker relocated to a distant rooftop (relatively stable but weather vulnerable and not recommended for permanent markers). These cases highlight that marker stability of directional markers is crucial.

Data availability

All raw data can be provided by the corresponding authors upon request.

275 Author contribution

YH and XZ initiated the study. SZ and QL designed the analysis methods. FY, SH and PG carried them out. YH prepared the manuscript with contributions from all coauthors.

Competing Interests

The authors have no competing interests to declare.

280 Acknowledgements

We express our gratitude to the colleagues at Hongshan geomagnetic observatory, Quanzhou geomagnetic observatory, and Yulin geomagnetic observatory for their assistance during the azimuth remeasurement process, which enabled the smooth completion of the survey work.

Funding Information

285 Supported by National Key R&D Program of China (2023YFC3007404); National Natural Science Foundation of China (42374092); DI Magnetometer Comparison (0525205).

References

- Bracke, S., INTERMAGNET Operations Committee and Executive Council: INTERMAGNET Technical Reference Manual, Version 5.2.0, https://tech-man.intermagnet.org/_/downloads/en/stable/pdf/, Last accessed 20 May 2025.
- 290 Cheng P.G., Li J.P. and Yu X.H.: Software of analytic method for determining astronomical azimuth, Engineering of Surveying and Mapping, 5(4):44-50, 1996.
- China Earthquake Administration (CEA): Specification for the construction of seismic station: Geomagnetic station (in Chinese). DB/T 9–2004. Beijing: Seismological Publishing House. 2004.
- China Earthquake Administration (CEA): Technical specifications for digital seismic and precursor observation: Electromagnetic Observation (Trial Implementation) [M]. Beijing: Seismological Publishing House, 11-16, 2001.
- 295 Jankowski, J., and Sucksdorff, C.: Absolute magnetic measurement, in: Guide for magnetic measurements and observatory practice, IAGA, Warszawa, Poland, 87–102, 1996.



- Khanzadyan M. A. and Mazurkevich A.V.: Development of a method for measuring the astronomical azimuth using an electronic total station. E3S Web of Conferences, 310(03007), <https://doi.org/10.1051/e3sconf/202131003007>, 2021.
- Li S.M., Wang G.G. and Shen Z.F.: Theory, method and application of positioning and navigation of geomagnetic field, Gns World of China, 2023, 48(6): 42-51. DOI: 10.12265/j.gnss.2023141,2023.
- Li Q.H., Xin C.J., Xu K.S., Shu L. and Gao H.H.: Application of differential GPS to the geographic azimuth measurement in China geomagnetic field monitoring network, China Earthquake Engineering Journal, 37(3):863-866, DOI:10.3969/ji.ssn.1000-0844.2015.03.0862, 2015.
- Lin Y, Sun J.J. and Yang X.: A review of the principles and methods of geomagnetic navigation and positioning technology, Gns World of China, 48(6): 32-41, DOI: 10.12265/j.gnss.2023134, 2023.
- Liu X.J., Zhegn Y. and Li C.H.: Precise determination of astronomical azimuth by hour angle method of multiple meridian stars. ACTA ASTRONOMICA SINICA,61(3):1-10, doi:10.15940/j.cnki.0001-5245.2020.03.008, 2020.
- Lu Y., Wei D.Y., Ji X.C. and Yuan H.: Review of geomagnetic positioning method, Navigation Positioning& Timing, 9(2):118-130, doi:10.19306/j.cnki.2095-8110.2022.02.015, 2022.
- Ma H.B.: Derivation of formulas for astronomical azimuth determination and approach to the method, Journal of Shenyang Institute of Gold Technology, 14(3):331-336,1995.
- Shi J.G.: Surveying data transmission method in drilling, Petroleum Drilling Techniques, 36(4):15-17, 2008.
- State Bureau of Quality and Technical Supervision (SBQTS): Specification for the geodetic astronomy, GB/T 17943-2000, <https://openstd.samr.gov.cn> (last access: 26 May 2025), 2000.
- St-Louis, B., INTERMAGNET Operations Committee and INTERMAGNET Executive Council: INTERMAGNET Technical Reference Manual, Version 5.1.1, (INTERMAGNET), Potsdam: GFZ Data Services, 134 p. <https://doi.org/10.48440/INTERMAGNET.2024.001>, Last accessed 20 May 2025.
- Wang Z. Y., Jiang H. and Hou Y.J.: Azimuth angle measurement of Dalian geomagnetic station, Azimuth angle measurement of Dalian Geomagnetic Station, Seismological and Geomagnetic Observation and Research, 35(5/6):120-123, doi:10.3969/j.issn.1003-3246.2014.05/06.023.2014.
- Xu X.G., Shang X.Q. and Zhou J.P.: Measurement of astronomic azimuth angle in Jinghai station and its quality evaluation, Northwestern Seismological Journal, 25(3): 281-285,2003.
- Yang F. X., Yang X., Zhang X. Y. and Huang J. M.: Azimuth survey of Urumqi geomagnetic station marker, Inland Earthquake,22(4):306-313,2008.
- Yin W.T.: Obtaining the azimuth with GPS, Geomatics & SpatialInformationTechnology,31(1):120-126, 2008.
- Yu J.K., Zhao R.R. and Ren Y.C.: Directional azimuth of GNSS calculation method, Journal of Navigation and Positioning, 6(1):120-122, doi:10.16547/j.cnki.10-1096.20180122, 2018.
- Zhou J.P., Huang W.B., Cheng A.L., et al.: Azimuth measurement and error analysis at Beijing geomagnetic observatory, Seismological and Geomagnetic Observation and Research,18(6):73-79,1997.



Zhou Y. T., Li Y. G. and Shang Q. F.: Study on the calibration method for the difference GPS direction, *Journal of Astronautic Metrology and Measurement*, 29(4):50-53, 2009.

335 Zhang H.B., Lian Q., Kang C.K. and Zhou J.: uantitative analysis of the relationship between geomagnetic anomaly and geological structure, *Geological and Mineral Surveying and Mapping*, 7(6): DOI:10.12238/gmsm.v7i6.1847, 2024a.

Zhang, S. Q., Fu, C. H., He, Y. F., Yang, D. M., Li, Q., Zhao, X. D., and Wang, J. J.: Quality control of observation data by the Geomagnetic Network of China, *Data Science Journal*, 15, 1–12, DOI:<http://dx.doi.org/10.5334/dsj-2016-015>, 2016.

340 Zhang, S. Q., Fu, C. H., Zhao, X. D., Zhang, X. X., He, Y. F., Li, Q., Chen, J., Wang, J. J., and Zhao, Q.: Strategies in the Quality Assurance of Geomagnetic Observation Data in China, *Data Science Journal*, 23, 1–11, DOI: <https://doi.org/10.5334/dsj2024-009>, 2024b.